International Journal of Applied Mathematics and Theoretical Physics
2021; 7(1): 1-9
http://www.sciencepublishinggroup.com/j/ijamtp
doi: 10.11648/j.ijamtp.20210701.11
ISSN: 2575-5919 (Print); ISSN: 2575-5927 (Online)

Optical Model Analysis of Elastic Scattering of $^{16}O + {}^{12}C$

Isaiah Ochala

Department of Physics, Faculty of Natural Sciences, Kogi State University, Anyigba, Nigeria

Email address:
ojoagbamiisaiah1234@gmail.com

To cite this article:
Isaiah Ochala. Optical Model Analysis of Elastic Scattering of $^{16}O + {}^{12}C$. *International Journal of Applied Mathematics and Theoretical Physics*. Vol. 7, No. 1, 2021, pp. 1-9. doi: 10.11648/j.ijamtp.20210701.11

Received: July 30, 2020; **Accepted**: August 28, 2020; **Published**: January 22, 2021

Abstract: This paper presents the optical model analysis of the elastic scattering of $^{16}O + {}^{12}C$ at the incident energies of 608 and 1503 MeV using optical potentials derived from B3Y-Fetal effective interaction. Optical model (OM) analysis of the elastic data of this system at these incident energies has shown two of the four optical potentials, the DDB3Y1-Fetal (K=176 MeV) and BDB3Y1-Fetal (K=235 MeV), to give a better description of the elastic data than the BDB3Y2-and BDB3Y3-Fetal potentials, making them the best-fit folded potentials, in agreement with previous work done with the M3Y-Reid effective interaction in both identical and non-identical heavy ions. This is a conclusive and convincing confirmation of the concensus among Nuclear Physics scholars, based on OM analyses of heavy ions, that nuclear matter has an underlying soft equation of state. In addition, results of calculations herein have also shown the best-fit folded potentials, the DDB3Y1-and BDB3Y1-Fetal with-227.8 and-220.6 MeV at 608 MeV and-124.3 MeV and-120.5 MeV at 1503 MeV, respectively as the largest values at smaller inter-nuclear distances, to be in good agreement with their counterparts, the DDM3Y1-Reid and BDM3Y1-Reid, whose largest values at smaller inter-nuclear distances are-231.6 and-223.8 MeV at 608 MeV and-138.8 MeV and-134.2 MeV at 1503 MeV respectively, in terms of magnitude, shape and trend. This is a further validation of the viability of the B3Y-Fetal, corroborating the findings of previous studies carried out with it. In the final analysis, the findings of this study have not shown the occurrence of distinctive features of refractive scattering such as Airy minima in the calculated cross sections at both 608 MeV and 1503 MeV in agreement with previous work.

Keywords: Optical Model, Folded Potentials, Elastic Scattering, Non-identical Heavy Ions, B3Y-Fetal Effective Interaction

1. Introduction

Optical potential is a potential that represents the interaction between a nucleon or a group of nucleons and a target nucleus [1]. It is a fundamental tool, used for many decades for the analysis of nuclear reactions, that enables elastic cross-sections over a wide range of ions, ion beam energies and scattering angles to be calculated [2, 3]. In many optical-model studies, the optical potential is constructed by theoretical and phenomenological methods. The former uses the fundamental theory of nucleon-nucleon interaction to solve the many-body problem of nucleon-nucleon or nucleus-nucleus interaction, whereas the latter starts from a physically reasonable form for the potential and adjusts its parameters systematically to optimize the fit to the experimental data. The theoretical method has the disadvantage of formidable mathematical difficulties, but is successful in giving an overall quantitative picture of the optical potential through a number of approximations. The phenomenological method has the advantage of giving a very good fit to experimental data by varying parameter sets, but is unsatisfactory on grounds that many different potentials can be found which give acceptable fits to the data. Therefore, to have a satisfactory potential, the two approaches are combined so that the fundamental theories give the overall form of the potential and the phenomenological method determines the optimum parameters of the potential. The parameters of the composite potential usually vary smoothly with energy and are similar for neighbouring nuclei. The origin of an erratic variation of the parameters for different nuclei can be traced to the differences in their structure, especially in collective states [4].

Generally, this optical potential is complex, having real and imaginary components. The real component accounts for elastic scattering while the imaginary component, arising from phenomenological method, represents non-elastic processes which cause the absorption of incident particles in nuclear reactions [1, 2, 5]. The convenient parameterization of the imaginary component is the Fermi distribution, which, in the context of the optical model, is referred to as the Woods-Saxon form, whereas the real component is represented by a folding-model potential in many theoretical optical model (OM) studies [4, 6, 7]. Since this study is a theoretical analysis of heavy-ion nucleus-nucleus elastic scattering, the real component is represented by a double folding potential in this work [8]. Such a folded potential is more frequently used for the study of α-particle as well as heavy-ion (HI) scattering because it gives a better representation of the surface part of the optical potential than the phenomenological potentials [1].

For the analysis of the elastic scattering of light heavy ions, the double folding model, with an effective interaction appropriately adjusted to nuclear matter properties, enters the OM analyses as a mean-field effect which is, indeed, very deep. It is well-known that heavy-ion collisions are usually accompanied by strong absorption, making the elastic scattering data sensitive only to the surface part of the nucleus-nucleus potential. However, lately, ever-increasing understanding of the interaction between heavy ions arising from studies of elastic scattering has shown certain combinations of heavy ions, for which absorption is relatively weak, to exhibit refractive scattering at incident energies of a few MeV per nucleon [7, 9, 10, 11]. One key advantage of refractive scattering is that it makes the determination of HI optical potential up to small internuclear distances possible, giving room for the possibility of testing different theoretical models for HI optical potentials by analyzing these systems (heavy ions) [12, 13]. This refractive scattering has been a subject matter of increased attention in the last two decades; and it has been established that only deep potentials, such as those generated by double folding model, are needed to describe the systematics of heavy-ion scattering.

So far, experimental evidence of refractive scattering has been found mainly in $^{12}C + ^{12}C$, $^{16}O + ^{16}O$ and $^{16}O + ^{12}C$ systems [9, 14]. Their elastic scattering angular distributions reveal unmistakable refractive features, such as rainbow scattering patterns and broad interference minima called "Airy minima" [10]. It is now known that these refractive features can be described consistently by optical potentials with deep (several hundreds MeV) real parts. Therefore, the clear observation of rainbow scattering features in $^{12}C + ^{12}C$, $^{16}O + ^{16}O$ and $^{16}O + ^{12}C$ elastic scattering data has definitely and particularly established that the real part of the light heavy-ion optical potential is strongly attractive and deep; and the imaginary part of the potential is weak enough to minimize absorption. Undoubtedly, a combination of these two features-deep real optical potential and incomplete absorption-makes possible the observation in the elastic angular distribution of distinctive refractive effects such as Airy minima superimposed on more classical diffractive features [7, 9].

This refractive behaviour has been conspicuously observed in the systematic analysis of the $^{16}O + ^{16}O$ system carried out by Nicoli et al. [15] at incident energies between 75 and 124 MeV and by Khoa et al. [9, 13] between 124 and 1120 MeV; and of the $^{16}O + ^{12}C$ system by Nicoli et al. [16] between 62 and 124 MeV and by Oglobin et al. [17] at 132 MeV [12]. In the systematic analysis of the $^{12}C + ^{12}C$ data at 14 energies between 71 and 127 MeV, refractive effects were not observed in the elastic data, so they concluded that only deep real potentials could describe the data [18]. Khoa et al. [9] did an extensive analysis of the elastic data for the same system at incident energies between 112 and 1016 MeV with the deep real potential generated by the double folding model and observed distinctive refractive features in the elastic scattering angular distribution.

Attempts have been made to extend the methods and approaches of previous researches to heavier projectile-target combinations, but absorption has consistently been observed to increase rapidly with the masses of the colliding nuclei, damping the nuclear reaction unfavourably. Thus, for the $^{20}Ne + ^{12}C$ system, only pure diffraction was observed and the system was dubbed "strongly absorbing" [19]. Also, previous experiments aimed at observing rainbow or at least refractive scattering in the $^{16}O + ^{20}Ca$ system at incident energies of 281 and 704 MeV failed to see any signatures of such effects [20]. Only at the energy of 214 MeV was what seemed to be a semblance or signature of nuclear rainbow observed at 45° in the angular distribution of the elastic cross-section as a "minimum" [20].

While efforts continue to be made to establish clear signatures of rainbow scattering in heavier systems, it is still, no doubt, a seriously contemplated idea among nuclear Physicists to find the possibility of observing refractive scattering at higher incident energies in those systems that are known to exhibit weak absorption so far. New theoretical models which might be used for better studies of elastic scattering may be developed in the future. However, within the confines of this study, the newly developed B3Y-Fetal is to be applied to the folding analysis of $^{16}O + ^{12}C$ at the incident energies of 608 and 1503 MeV within the framework of optical model in anticipation that the expected results will show signs of refractive scattering as well give a good insight into distinctive qualities of the new effective interaction among numerous theoretical models for heavy-ion optical potential. For comparative purposes, the new effective interaction is used alongside the M3Y-Reid effective interaction in this work.

The organization of this paper is such that Section 2.0 discusses briefly the double folding procedure, which is followed by presentation and discussion of results of the study in Section 3.0; and Section 4.0 is devoted to concluding remarks.

2. Double Folding Procedure

In a bid to study the elastic scattering of $^{16}O + ^{12}C$ nuclear system at the incident energies of 608 and 1503 MeV, a nucleus-nucleus optical potential is constructed which is composed of the double folding model as the real part while the imaginary part is parameterized phenomenologically as a two-parameter Woods-Saxon shape.

The basic inputs to the double folding model calculation are the nuclear densities of the colliding nuclei and a realistic effective nucleon-nucleon (NN) interaction which reproduces the basic nuclear matter properties as well as the density and energy dependence of the nucleon optical potential. Here, the effective interaction of particular interest is the B3Y-Fetal interaction, derived on the basis of the lowest order constrained variational principle, whose radial form in terms of three Yukawa functions is [21]:

$$v^{D}(r)=\frac{10472.13e^{-4r}}{4r}-\frac{2203.11e^{-2.5r}}{2.5r}$$

$$v^{EX}(r)=\frac{499.63e^{-4r}}{4r}-\frac{1347.77e^{-2.5r}}{2.5r}-\frac{7.8474e^{-07072r}}{0.7072r} \quad (1)$$

The well-known M3Y-Reid interaction is also used along with the B3Y-Fetal interaction as a standard with which the latter is compared. For this reason, the explicit functional form of the M3Y-Reid NN interaction is expressed in terms of three Yukawas as [6, 7, 22]:

$$v^{D}(r)=\frac{7999.00e^{-4r}}{4r}-\frac{2134.25e^{-2.5r}}{2.5r}$$

$$v^{EX}(r)=\frac{4631.375e^{-4r}}{4r}-\frac{1787.125e^{-2.5r}}{2.5r}-\frac{7.8474e^{-07072r}}{0.7072r} \quad (2)$$

For the optical model analysis of the elastic scattering of the chosen nuclear systems, the B3Y-Fetal interaction is to be used in its density-and energy-dependent form:

$$v^{D(EX)}(E, \rho, r)=g(E)\,F(\rho)\,v^{D(EX)}(r), \quad (3)$$

where E is the incident nucleon energy, the energy dependence of the optical potential, g(E) ~ 1-0.002E for M3Y-Reid interaction [7, 9, 23] as well as B3Y-Fetal interaction [24] and F(ρ) is the density-dependent factor whose explicit forms are

$$F(\rho)=C_o\,(1+\alpha e^{-\beta\rho}) \quad (4)$$

and

$$F(\rho)=C_o\,(1+\alpha\rho^{\beta}) \quad (5)$$

representing the DDM3Yn (n=1) and BDM3Yn (n=0, 1, 2, 3) interactions respectively. Herein, the B3Y-Fetal effective interaction is used in the DDM3Y1, BDM3Y1, BDM3Y2 and BDM3Y3 density-dependent versions so that the resulting density-dependent B3Y-Fetal interactions are called the DDB3Y1-Fetal, BDB3Y1-Fetal, BDB3Y2-Fetal and BDB3Y3-Fetal interactions respectively.

In a test of viability, this new effective interaction was applied to the study of symmetric nuclear matter in an earlier work [25] in the named density dependences and was found to reproduce the saturation properties of this nuclear matter with results that were in excellent agreement with previous work done with M3Y-Reid and M3Y-Paris interactions [6, 7, 9]. Shown in Table 1 are the parameters of density dependence and incompressibility obtained with the B3Y-Fetal interaction in that paper.

Table 1. *Parameters of Density Dependence and Nuclear Incompressibility at Equilibrium Obtained with B3Y-Fetal Effective Interaction.*

Density Dependent Version	*C*	A	β	K [MeV]
DDB3Y1-Fetal	0.2986	3.1757	2.9605	176
DDB3Y0-Fetal	1.3045	1.0810	2/3	196
DDB3Y1-Fetal	1.1603	1.4626	1	235
DDB3Y2-Fetal	1.0160	4.9169	2	351
DDB3Y3-Fetal	0.9680	20.250	3	467

In this model, the direct and exchange parts of the nucleus-nucleus potential are obtained by folding the densities of the projectile and target nuclei with the direct and exchange components of the effective nucleon-nucleon (NN) interaction as presented in equations (6) and (7) respectively

$$V_D(E,R)=\int \rho_1(r_1)\rho_2(r_2)v^{D}\,(\rho,E,s)dr_1dr_2 \quad (6)$$

with $s=r_2-r_1+R$

$$V_{EX}(E,R)=\int \rho_1(r_1,r_1+s)\rho_2(r_2,r_2-s)v^{EX}\times exp\frac{[iK(R)s]}{M}dr_1dr_2 \quad (7)$$

where ρ_1 and ρ_2 are the densities of the interacting nuclei. The exchange term is non-local due to the effect of anti-symmetrization occasioned by the single-nucleon knock-on exchange. To solve the non-locality problem, an exact, consistent microscopic approximation to the exchange potential, instead of the semi-phenomenological zero-range approach, developed by Khoa *et al*. [6, 7, 9, 26] is adopted in this work. Their approach produces an accurate local approximation, resulting from treating the relative motion locally as a plane wave so that k(R) in equation (7) is the local momentum of relative motion represented by:

$$K^2(R)=\frac{2mM}{\hbar^2}[E_{c.m}-V(E,R)-V_C(R)] \quad (8)$$

where $M=A_1A_2/(A_1+A_2)$ is the reduced mass, $E_{c.m}$ the centre-of-mass (c.m) energy, E the incident laboratory energy per nucleon and m the bare nucleon mass. $V(E,R)=V_D(E,R)+V_{EX}(E,R)$ is the total nuclear potential and $V_C(R)$ is the Coulomb potential.

In this work, the exchange potential is evaluated by exact iterative method; and the energy dependence of the total folded potential, V (E, R) on the exchange term which is much stronger than the energy dependence denoted by g (E), is obtained from the real folded optical potential through accurate evaluation of the knock-on exchange effects [6, 11, 27]. A very important parameter which gives insight into the energy dependence of the optical potential is the volume integral of the folded potential per interacting nucleon pair expressed as [7, 9, 27]:

$$J_R(E) = \frac{4\pi N_R}{A_1 A_2}\int_0^\infty [V_D(E,r) + V_{EX}(E,r)]r^2 dr \quad (9)$$

As a measure of the potential strength, it can be used to distinguish a family of real folded potentials [14].

Essentially, the double-folding procedure generates the real part of the nucleus-nucleus optical potential, supplemented by an imaginary potential which accounts for absorption into non-elastic channels. This hybrid approach, composed of the folding model as the real component and a standard Woods-Saxon (WS) potential as the imaginary component of the optical potential, is used for the optical-model (OM) analysis of elastic scattering in this study. In totality, the optical potential is:

$$U(E,R) = V(E,R) + iW(E,R) \quad (10)$$

where the real and imaginary parts of the optical potential are:

$$V(E,R) = N_R[V_D(E,R) + V_{EX}(E,R)] \quad (11)$$

and

$$W(E,R) = \frac{-W_V}{1 + exp\left(\frac{(R-R_W)}{a_W}\right)} \quad (12)$$

where N_R is the normalization factor for the real (folded) potential adjusted appropriately to fit the elastic data alongside the parameters W_v, R_W and a_W which are the strength, radius and diffuseness of the Woods-Saxon function [28]. All the nuclear densities in the folding model are taken as a Fermi distribution with parameters that can reproduce the shell-model densities for the nuclei under consideration; and all computational analyses of the optical model are carried out in the present work using the ECIS-97 code.

To study the energy dependence of the real heavy ion potential, efforts were made in previous work to plot all N_R and J_R values obtained by using one of the best-fit real folded potentials, the DDB3Y1-Fetal, in the analyses of ^{16}O and ^{12}C [24, 30] scattering data against the incident energy. The plots are reproduced in the upper and lower regions, respectively, of Figure 1. The folding model used for the nucleus-nucleus potential therein was adjudged satisfactorily realistic as the plot in the upper region has shown N_R to depend weakly on energy and vary around a value of 0.9 [7, 9, 24, 30]. The folding results have additionally established the intrinsic energy dependence arising from the exchange effects and the weak explicit energy dependence g(E) factor introduced into the effective NN interaction (Equation (3)) as the main sources of the total energy dependence of the real HI optical potential [9, 24, 30].

In the lower region of Figure 1, the volume integral of the real folded potential per interacting nucleon pair, J_R is seen to decrease smoothly from about 340 MeV/m^3 to 150 MeV/m^3 as the incident energy increases from about 10 to 120 MeV/nucleon. This trend is known to agree well with previous work [9], validating the prediction of the energy dependence of the real HI potential by the folding model in that work to be reliably satisfactory. It is with this confidence that the same folding model is used in this work for the analysis of the elastic data of the non-identical ^{16}O + ^{12}C system.

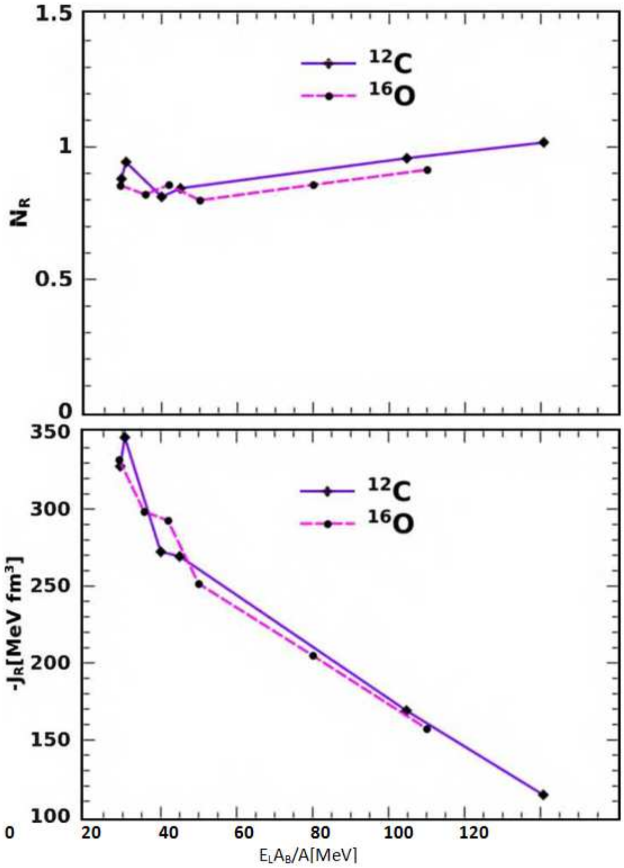

Figure 1. The Energy Dependence of the Renormalization Factor, N_R (upper part) and the volume integral, Jr (lower part) of the DDB3Y1-FETAL Potential Deduced from the Folding Analyses of the Elastic ^{16}O and ^{12}C Scattering Data at Energies up to 120 MeV/nucleon.

3. Results and Discussion

This work essentially represents the application of the new M3Y-type effective interaction, the B3Y-Fetal, to optical model analyses of the elastic scattering of ^{16}O + ^{12}C at E_{lab}=608 and 1503 MeV. The results of calculations of the real optical potential for ^{16}O + ^{12}C scattering at E_{lab}=608 and 1503 MeV alongside the calculated cross sections are shown in Table 2 and Figures 2-7. The heavy-ion optical potential derived from the B3Y-Fetal has been found to demonstrate weak absorption in the chosen nuclear system. The results show the optical potentials derived from the B3Y-Fetal effective interaction to be in good agreement with the optical potentials based on the M3Y-Reid effective interaction.

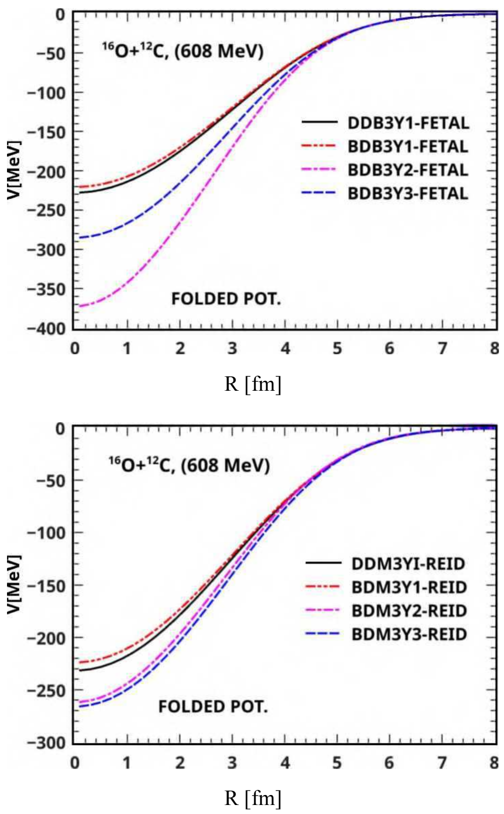

Figure 2. *Real Optical Potentials for ^{16}O + ^{12}C Based on B3Y-Fetal (Upper Part) and M3Y-Reid (Lower Part) Obtained at the Incident Energy of 608 MeV.*

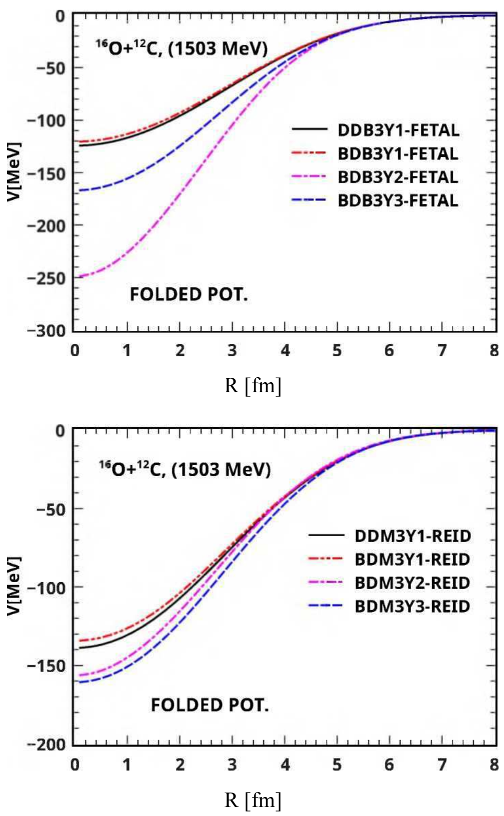

Figure 3. *Real Optical Potentials for ^{16}O + ^{12}C Based on B3Y-Fetal (Upper Part) and M3Y-Reid (Lower Part) Obtained at the Incident Energy of 1503 MeV.*

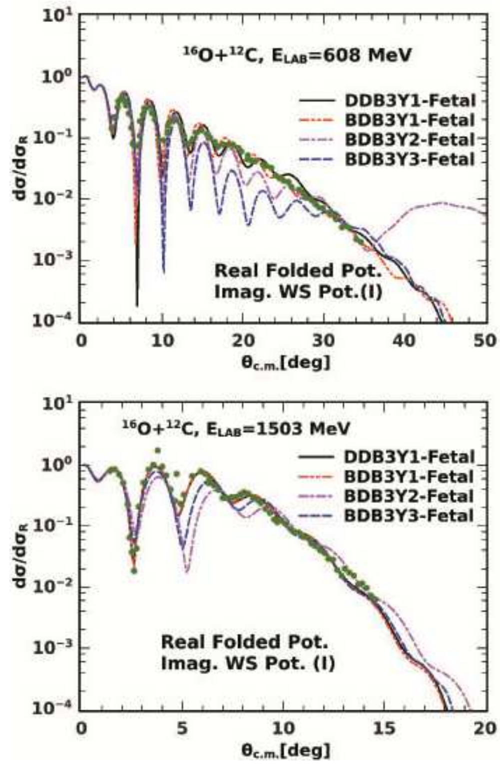

Figure 4. *Fits to the ^{16}O + ^{12}C Elastic Data at E_{Lab}=608 MeV (Upper Part) and 1503 MeV (Lower Part) Based on B3Y-Fetal obtained with Real Folded and Volume Woods-Saxon [W(R)=WS(I)] Imaginary Potentials.*

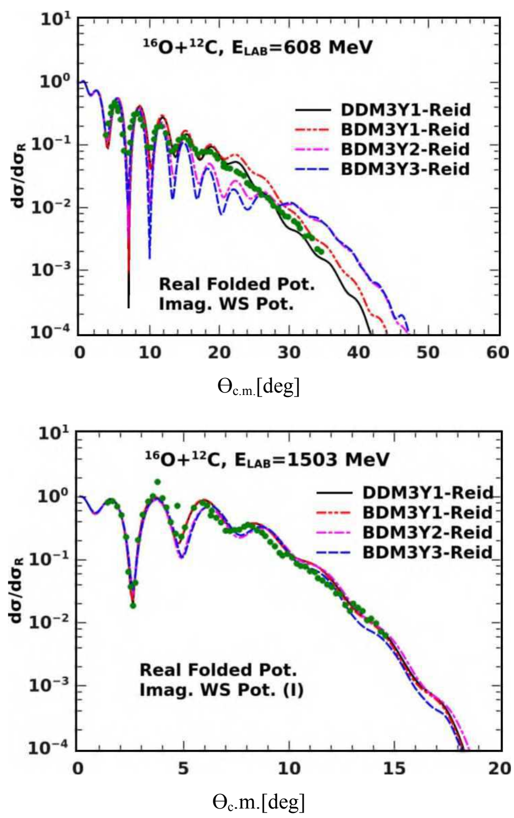

Figure 5. *Fits to the ^{16}O + ^{12}C Elastic Data at E_{Lab}=608 MeV (Upper Part) and 1503 MeV (Lower Part) Based on M3Y-Reid obtained with Real Folded and Volume Woods-Saxon [W(R)=WS(I)] Imaginary Potentials.*

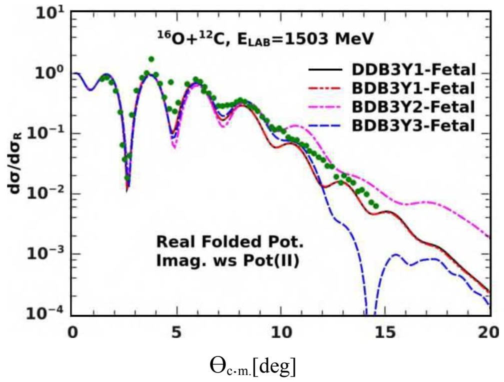

Figure 6. *Fits to the $^{16}O + ^{12}C$ Elastic Data at E_{Lab}=1503 MeV Based on B3Y-Fetal Obtained with the Real Folded and Volume Woods-Saxon [W(R)=WS(II)] Imaginary Potentials.*

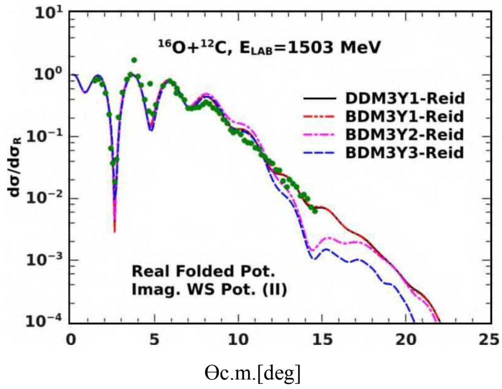

Figure 7. *Fits to the $^{16}O + ^{12}C$ Elastic Data at E_{Lab}=1503 MeV Based on M3Y-Reid Obtained with the Real Folded and Volume Woods-Saxon [W(R)=WS(II)] Imaginary Potentials.*

Table 2. *Optical Parameters Used in the Folding Analyses of the Elastic Data of $^{16}O + ^{12}C$ at E_{Lab}=608 and 1503 MeV. (Imaginary potential has a volume WS shape). Results obtained in Ref. [9] with the M3Y-Reid interaction are in brackets.*

(a) $^{16}O + ^{12}C$, E_{Lab}=608 MeV

Potential	N_r	$-J_r$ (MeV fm^3)	$\langle r_R^2\rangle^{1/2}$ (fm)	W_V (MeV)	R_W(fm)	a_W (fm)	σ_r (mb)	χ^2
DDM3Y1-REID	0.7930	235.1	4.0462	27.693	5.3460	0.6109	1377	22.4
	(0.8341)	(233.0)	(4.0218)	(25.528)	(5.3465)	(0.6109)	(1350)	(7.0)
DDB3Y1-FETAL	0.8061	230.5	4.0133	27.2314	5.3465	0.6109	1371	24.9
BDM3Y1-REID	0.8533	247.7	4.0505	27.496	5.3801	0.6092	1388	31.9
	(0.8503)	(232.3)	(4.0277)	(24.996)	(5.3831)	(0.6092)	(1357)	(8.2)
BDB3Y1-FETAL	0.8533	239.2	4.0166	27.496	5.3801	0.6092	1386	27.2
BDM3Y2-REID	0.8356	255.3	3.9556	28.992	5.4672	0.6097	1437	43.3
	(0.8894)	(231.1)	(4.0475)	(23.758)	(5.4672)	(0.6097)	(1381)	(11.7)
BDB3Y2-FETAL	0.8831	320.9	3.7864	28.992	5.4672	0.6097	1437	39.1
BDM3Y3-REID	0.8221	262.8	3.9440	28.954	5.5744	0.6251	1501	47.2
	(0.9505)	(230.1)	(4.1026)	(21.554)	(5.6744)	(0.6251)	(1451)	(17.5)
BDB3Y3-FETAL	0.7665	248.1	3.9090	28.954	5.5744	0.6251	1498	46.9

(b) $^{16}O + ^{12}C$, E_{Lab}=1503 MeV WSI Pot. Note: r, v and w are subscripts referring to real, volume and Woods-Saxon potential component respectively.

Potential	N_r	$-J_r$ (MeV fm^3)	$\langle r_R^2\rangle^{1/2}$ (fm)	W_V (MeV)	R_W (fm)	a_W (fm)	σ_r (mb)	χ^2
DDM3Y1-REID	0.8660	159.3	4.1234	16.440	5.6629	0.7741	1329	7.5
	(0.8699)	(164.5)	(4.1204)	(16.240)	(5.6629)	(0.7741)	(1323)	(9.0)
DDB3Y1-FETAL	0.8699	142.3	4.1103	16.240	5.6629	0.7741	1322	18.9
BDM3Y1-REID	0.8905	160.0	44.1296	15.967	5.7248	0.7688	1337	7.2
	(0.8905)	(164.4)	(4.1272)	(15.767)	(5.7248)	(0.7688)	(1331)	(7.8)
BDB3Y1-FETAL	0.8905	142.6	4.1152	15.767	5.7248	0.7688	1328	29.9
BDM3Y2-REID	0.7766	143.2	4.0390	15.190	5.8517	0.7528	1351	12.8
	(0.9413)	(164.9)	(4.1492)	(14.731)	(5.8717)	(0.7528)	(1347)	(6.2)
BDB3Y2-FETAL	0.5077	114.5	3.7915	16.620	5.7517	0.7528	1348	58.5
BDM3Y3-REID	0.6854	136.2	4.0168	13.1473	6.1234	0.7291	1376	11.4
	(1.0234)	(166.3)	(4.2071)	(13.078)	(6.1233)	(0.7291)	(1376)	(10.4)
BDB3Y3-FETAL	0.6797	129.8	3.9858	14.198	6.1230	0.7270	1414	20.0

(c) $^{16}O + ^{12}C$, E_{Lab}=1503MeV WSII Pot.

Potential	N_r	$-J_r$ (MeV fm^3)	$\langle r_R^2\rangle^{1/2}$ (fm)	W_V (MeV)	R_W (fm)	a_W (fm)	σ_r (mb)	χ^2
DDM3Y1-REID	1.0913	200.7	4.1234	44.829	4.8051	0.6097	1179	8.6
	(1.0913)	(206.3)	(4.1204)	(44.629)	(4.8051)	(0.6097)	(1178)	(13.4)
DDB3Y1-FETAL	1.0913	178.5	4.1103	44.829	4.8051	0.6097	1177	17.7
BDM3Y1-REID	1.1068	198.9	4.1296	44.458	4.7992	0.6142	1180	8.5
	(1.1068)	(204.4)	(4.1272)	(44.258)	(4.7992)	(0.6142)	(1179)	(13.2)
BDB3Y1-FETAL	1.1068	177.2	4.1152	44.458	4.7992	0.6142	1178	17.7
BDM3Y2-REID	1.1398	210.1	4.0390	43.461	4.7822	0.6272	1181	18.8
	(1.1398)	(199.7)	(4.1492)	(43.261)	(4.7822)	(0.6272)	(1180)	(12.2)
BDB3Y2-FETAL	0.9398	211.9	3.7915	43.261	4.7822	0.6272	1177	34.0
BDM3Y3-REID	0.9798	194.7	4.0168	41.312	4.7362	0.6600	1185	18.7
	(1.1798)	(191.7)	(4.2071)	(41.312)	(4.7362)	(0.6600)	(1186)	(9.7)
BDB3Y3-FETAL	0.9798	187.1	3.9858	41.312	4.7362	0.6600	1183	32.0

3.1. The Real Folded Potential

The four real folded potentials, derived from the B3Y-Fetal effective interaction and used in this work-the DDB3Y1-Fetal, BDB3Y1-Fetal, BDB3Y2-Fetal and BDB3Y3-Fetal-are shown in the upper regions of Figures 2 and 3 along with the M3Y-Reid-based DDM3Y1-Reid, BDM3Y1-Reid, BDM3Y2-Reid and BDM3Y3-Reid potentials in the lower regions. lt is quite informative to note that the first two optical potentials (DDM3Y1-Reid and BDM3Y1-Reid) in the lower regions of Figures 2 and 3, being close in magnitude, are widely separated from the last two optical potentials (BDM3Y2-Reid and BDM3Y3-Reid), which are also shown to be close in magnitude. This wide separation between the two sets of optical potentials appears to be a sharp demarcation that puts them in two classes that are manifested in their description of the elastic data of the system under consideration. The same sharp demarcation is also illustrated in the upper regions of these Figures where the B3Y-Fetal-based potentials are found.

Generally, the agreement of the potentials based on the B3Y-Fetal with the potentials derived from the M3Y-Reid effective interaction in terms of magnitude, shape and trend is impressive. In terms of magnitude, results of folding calculations have shown the largest values of DDB3Y1-Fetal, BDB3Y1-Fetal, BDB3Y2-Fetal and BDB3Y3-Fetal potentials at smaller inter-nuclear distances to be-227.8,-220.6,-372.2 and-285.0 MeV at the incident energy of 608 MeV and-124.3,-120.5,-248.7 and-166.9 MeV at the incident energy of 1503 MeV respectively; whereas the largest values of DDM3Y1-Reid, BDM3Y1-Reid, BDM3Y2-Reid and BDM3Y3-Reid potentials are-231.6,-223.8,-261.8 and-265.9 MeV at the incident energy of 608 MeV and-138.8,-134.2,-156.3 and-160.7 MeV at the incident energy of 1503 MeV respectively. Here, the differences between the DDB3Y1-Fetal and BDB3Y1-Fetal at 608 and 1503 MeV are-7.2 MeV and-3.8 MeV respectively while the differences between DDM3Y1-Reid and BDM3Y1-Reid at these energies are-7.8 MeV and 4.6 MeV respectively. This shows that the B3Y-Fetal is in excellent agreement with the M3Y-Reid effective interaction. The BDB3Y2-Fetal potential is seen in this non-identical (^{16}O + ^{12}C) system to have a much larger value than the BDB3Y3-Fetal potential; this unusual behaviour is not exhibited in identical systems such as ^{12}C + ^{12}C [29] and ^{16}O + ^{16}O [30]. As regards trend, each real folded potential based on the B3Y-Fetal or M3Y-Reid becomes repulsive as the incident energy increases from 608 MeV to 1503 MeV in Figures 2 and 3 in conformity with the well-established trend in [9].

3.2. Fits to ^{16}O + ^{12}C Elastic Data

In the present work, the elastic scattering of ^{16}O + ^{12}C system is studied at the energies of 608 MeV and 1503 MeV respectively. The graphical representation of the elastic cross sections obtained with the four folded potentials is given in Figures 4-7 while the optical parameters are presented in Table 2. The fit to the data at 608 MeV was done using the weak WSI potential, but for the fit to the data at 1503 MeV, two sets of the imaginary potential were used: a weak one (WSI) with a depth of about 16 MeV and a strong one (WSII) about 50 MeV deep.

Figure 4 shows clearly that the DDB3Y1-Fetal and BDB3Y1-Fetal potentials give a better description of the data with the weak WSI potential (minimal absorption) at both 608 MeV and 1503 MeV than the BDB3Y2-Fetal and BDB3Y3-Fetal potentials. This is in agreement with previous work [9] and the results for ^{12}C + ^{12}C [29] and ^{16}O + ^{16}O [30] systems in which DDM3Y1-Reid and BDM3Y1-Reid as well as DDB3Y1-Fetal and BDB3Y1-Fetal were described as the best-fit folded potentials. Figure 5 has been included to show that the optical potentials based on B3Y-Fetal and M3Y-Reid are in agreement. Herein, the distinctive features of refractive scattering such as Airy minima are not observed in the calculated cross sections obtained with the M3Y-Reid and B3Y-Fetal optical potentials at both incident energies; the sensitivity of the elastic data at either energy to the real optical potential at small inter-nuclear distances is not pronounced.

Folding results at 1503 MeV show that the real folded potentials have better fits to the data with WSII imaginary potential than with the WSI potential (Tables 2b and 2c). For the data at 1503 MeV in heavy absorption conditions, the DDB3Y1-Fetal and BDB3Y1-Fetal have exactly the same fit while the BDB3Y2-Fetal and BDB3Y3-Fetal have about the same fit as shown in Table 2c and Figures 6 and 7. Furthermore, the renormalization factors, N_R for the best-fit folded potentials, DDB3Y1-Fetal and BDB3Y1-Fetal as well as DDM3Y1-Reid and BDM3Y1-Reid in the heavy-absorption case are found in Table 2c to be greater than unity contrary to the systematic behaviour of the best-fit real folded potentials seen so far in the present work and in the elastic scattering of ^{12}C + ^{12}C and ^{16}O + ^{16}O systems [9, 29, 30]; and this suggests strongly that the results for this system at 1503 MeV for the weak-absorption imaginary potential (WSI) might be more relevant.

In summary, this version of heavy-ion optical potential, based on B3Y-Fetal, applied to the study of the elastic scattering of ^{16}O + ^{16}C system has demonstrated weak absorption in the cases considered in this work. Finally, for the sake of emphasis, it has to be said that the c, which nsistent agreement of DDB3Y1-Fetal and BDB3Y1-Fetal [24, 25, 29, 30] or DDM3Y1-Reid and BDM3Y1-Reid [9] potentials, as best-fit folded potentials, in the description of the elastic data of ^{12}C + ^{12}C and ^{16}O + ^{16}O systems, which is also observed in the present work is a convincing pointer to the concensus among Nuclear Physics scholars that the cold nuclear matter is governed by a soft equation of state [9]. Figures 2 and 3 clearly separate the best-fit folded potentials, being very close in magnitude, from the BDM3Y2-and BDM3Y3-Reid or BDB3Y2-and BDB3Y3-Fetal, which appear to be in a separate group of potentials with poor description of elastic data, known to represent “stiff” equation of state [9, 31].

4. Conclusion

In this study, the folding analysis of the elastic scattering of $^{16}O + ^{12}C$ has been carried out within the framework of optical model at the incident energies of 608 and 1503 MeV.

Some density dependences have been introduced into the B3Y-Fetal effective interaction to reproduce the saturation properties of normal nuclear matter within a Hartree-Fock scheme; and these have predicted the nuclear incompressibility K to have values ranging from 176 to 467 MeV. The B3Y-Fetal-based density dependent interactions have been used to calculate the real part of the heavy-ion optical potentials for the non-identical system studied herein. In this way, the optical model analyses have been used to probe the sensitivity of the scattering data to different forms of density dependence as well as to the various values of the associated incompressibility K of the cold nuclear matter. The results of this study have shown the DDB3Y1-Fetal and BDB3Y1-Fetal optical potentials to be the best-fit folded potentials; this confines a realistic K value to a range of about 176 to 235 MeV, which corresponds to a "soft" nuclear EOS. This study allows one to suggest the most realistic density dependent interaction that is currently available for the folding model calculations of nucleus-nucleus potentials. In addition, the results obtained in this work show clearly and particularly the importance of refractive nucleus-nucleus scattering experiments as a means to provide accurate data to test an effective interaction.

Clear signatures of refractive scattering such as Airy minima have not been observed in the calculated cross sections at the energies of interest in this work, but the B3Y-Fetal-based optical potentials have been found to demonstrate good agreement with the optical potentials derived from the M3Y-Reid effective interaction in the description of the elastic data of this system.

Finally, the findings of this study could find useful applications in Nuclear Astrophysics where nuclear EOS is a major ingredient in calculations of reaction rates for understanding primordial nucleosynthesis and hydrostatic burning in stars.

Acknowledgements

With profuse thanks, Professor D. T. Khoa of Institute for Nuclear Science and Technology, Vietnam, deserves a grateful mention for excellent and thorough guide provided through the optical model analysis with the best academic and human resources. The members of the Nuclear Physics Group and the Management of Institute for Nuclear Science and Technology, Vietnam are thankfully acknowledged for their immense and diverse contributions to the success of this work. The Nigerian Federal Government is greatly appreciated for the ETF and TETFund training intervention which provided enormous succour for this work.

References

[1] Hodgson, P. E. (1994). The Nucleon Optical Model. World Scientific Publishing Co. Ltd. London. 421P.

[2] Jackson, D. F. (1974). Nuclear Sizes and Optical Model. Rep. Prog. Physics. 37, 55-146.

[3] Pachouri, D., Rafi, S., and Haider, W. (2012). Microscopic Optical Potentials for Nucleon-Nucleus Scattering at 65 MeV. Journal of Physics G: Nuclear and Particle Physics. 39 (055101), 1-18.

[4] Glendenning, N. K. (2004). Direct Nuclear Reactions. World Scientific Publishing Co. Ltd., 5 Toh Tuck Link, Singapore. 378P.

[5] Hamada, S., Burtebayev, N., Gridnev, K. A. and Amangeldi, N. (2011). Further Investigation of the Elastic Scattering of ^{16}O, ^{14}N and ^{12}C on the Nucleus of ^{27}Al at Low Energies. PhysicaScripta. 84 (045201). 54-60.

[6] Khoa, D. T., Oertzen V. W. and Oglobin. (1996). Study of the Equation of State for Asymmetric Nuclear Matter and Interaction Potential between Neutron-Rich Nuclei Using the Density-Dependent M3Y Interaction. Nuclear Physics A. 602, 98-132.

[7] Khoa, D. T., Satchler, G. R. and Oertzen, W. V. (1997). Nuclear Incompress ibility and Density Dependent NN Interactions in the Folding Model for Nucleus Potentials. Physical Review C. 56 (2), 954-969.

[8] Carlson, V. B. (2000). Lectures Given at the Workshop on Nuclear Dataand Nuclear Reactors: Physics, Design and Safety. Brazil. 62-104.

[9] Khoa, D. T., Oertzen, V. W. and Bohlen, H. G. (1994). Double-Folding Model for Heavy-ion Optical Potential: Revised and Applied to Study ^{12}C and ^{16}O Elastic Scattering. Physical Review C. 49 (3), 1652-1667.

[10] Oertzen, V. W., Bohlen, H. G., Subbotin, V. and Khoa, T. D. (2001). Nuclear Rainbows, Nucleus-Nucleus Potentials and the EOS of Nuclear Matter. International Winter Meeting on Nuclear Physics. Bormio.

[11] Brandan, M. E. and Satchler, G. R. (1997). The Interaction between Light Heavy Ions and What It Tells Us. Physics Reports. 285, 143-243.

[12] Hamada, S., Burtebayev, N., Amangeldi, N., Gridnev, K. A., Rusek, K., Kerimkulov, Z. and Maltsev, N. (2012). Phenomenological and Semi-microscopic Analysis for ^{16}O and ^{12}C Elastically Scattering on the Nucleus of ^{16}O and ^{12}C at Energies Near Coulomb Barrier. Journal of Physics: Conference Series. 381 (12130). 1-6.

[13] Khoa, D. T., Oertzen, V. W., Bohlen, H. G. and Nuoffer, F. (2000). Study of Diffractive and Refractive Structure in the Elastic $^{16}O + ^{16}O$ Scattering at Incident Energies Ranging from 124 to 1120 MeV. Nuclear Physics A. 672, 387-416.

[14] Katsuma, M., Sakuragi, Y., Okabe, S. and Kondo, Y. (2002). Coupled-Channels Study of the Nuclear Rainbow Phenomenon for the $^{12}C + ^{16}O$ System. Progress of Theoretical Physics. 107 (2). 377-401.

[15] Nicoli, M. P., Haas, F., Freeman, R. M., Aissaoui, N., Beck, C., Elanique, A., Nouicer, R., Morsad, A., Suzana, S., Zoran, B., Brandan, E. M, Satchler, G. R. (1999). Elastic Scattering of ^{16}O + ^{16}O at Energies E/A Between 5 and 8 MeV. Physical Review C 60 (6), 064608.

[16] Nicoli, M. P., Haas, F., Freeman, R. M., Suzana, S., Zoran, B., Morsad, A., Satchler, G. R., Brandan, E. M. (2000). Detailed Study and Mean-field Interpretation of ^{16}O + ^{16}O Elastic Scattering at Seven Medium Energies. Physical Review C 61 (3), 034609.

[17] Ogloblin, A. A., Khoa, D. T., Kondo, Y., Glukhov, A. Y., Demyanova, A. S., Rozhkov, M. V., Satchler, G. R. and Goncharov, S. A. (1998). Prou-nounced Airy Structure in Elastic ^{16}O + ^{12}C Scattering at Elab=132 MeV. Physical Review C. 57 (4), 1797.

[18] Farid, M. E., Mahmoud, Z. M. M. and Hassan, G. S. (2001). Analysis of Heavy Ions Elastic Scattering Using the Double Folding Cluster Model. Nuclear Physics A. 691, 671-690.

[19] McVoy, W. K. and Chehime, H. (1994). Airy, Glauber and Pauli: What Can We Learn About In-Medium NN Interactions from Heavy-ion Scattering?. Revista Mexicana de Fisica. 40 (1), 144-154.

[20] Demyanova, A. S., Belov, E. S., Glukhov, A. Y., Goncharov, A. S., Izad-pankh, A., Khlebnikov, V. S., Maslov, A. V., Sobolev, G. Y., Oglobin, A. A., Penionzhkevich, E. Y., Trzaska, H. W., Tultsev, Y. A. and Tyurin, P. G.(2006). First Observation of Nuclear Rainbow Scattering in ^{16}O + ^{40}Ca. Proceedings of National Conference on Nuclear Physics. TOM 69 (8), 1-5.

[21] Fiase J. O., Devan K. R. S. and Hosaka A. (2002). Mass Dependence of M3Y-Type Interactions and the Effects of Tensor Correlations. Physical Review C. 66 (014004), 1-9.

[22] Bertsch, G., Borsowicz, J., McManus, H. and Love, W. G. (1977). Inter-actions for Inelastic Scattering Derived from Realistic Potentials. Nuclear Physics A. 284, 399-419.

[23] Khoa, D. T., Oertzen,, V. W. and Bohlen H. G. and Ohkubo, S. (2006). Nuclear Rainbow Scattering and Nucleus-Nucleus Potential. Journal of Physics: Nuclear Physics. 34 (3), 1-65.

[24] Ochala, I. (2016). Application of the New M3Y-Type Effective Interaction to Nuclear Matter and Optical Model Analyses. Unpublished PhD Thesis. Benue State University. Makurdi. 186P.

[25] Ochala, I. and Fiase J. O. (2018). Symmetric Nuclear Matter Calculations-A Variational Approach. Physical Review C. 98 (064001), 1-8.

[26] Khoa, D. T. and Satchler, G. R. (2000). Generalized Folding Model for Elastic and Inelastic Nucleus-Nucleus Scattering using Realistic Density-Dependent Nucleon-Nucleon Interaction. Nuclear Physics A. 668, 3-41.

[27] Satchler, G. R and Love, W. G. (1979). Folding Model Potentials from Realistic Interactions for Heavy-ion Scattering. Physics Reports (Review Section of Physics Letters). 55 (3), 183-254.

[28] Hamada, S., Burtebayev, N., Amar, A. and Amangeldi, N. (2010). Analysis of the Elastic Scattering of ^{12}C on ^{n}B at Energy Near Coulomb Barrier Using Different Optical Potential Codes. World Academy of Science, Engineering and Technology. 69. 54-68.

[29] Ochala, I., Terver D. and Fiase J. O. (2019a). A Study of ^{12}C + ^{12}C Nuclear Reaction Using a New M3Y-Type Effective Interaction. A Paper being Reviewed in International Journal of Physics Research and Applications, USA.

[30] Ochala, I. and Fiase J. O. (2019b). The B3Y-Fetal Effective Interaction in the Folding Analysis of Elastic Scattering of ^{16}O + ^{16}O. A Paper being Reviewed in European Physical Journal A, Bolonga.

[31] Basu, D. N., Chowdhury, P. R. and Samanta, C. (2006). Equation of State for Isospin Asymmetric Nuclear Matter Using Lane Potential. Acta Physica Polonica B. 37 (10), 2869–2887.